AISTech 2019 — Proceedings of the Iron & Steel Technology Conference
6–9 May 2019, Pittsburgh, Pa., USA
DOI 10.1000.377.223

Development of a Predictive Model for Minimizing Ladle Desulfurization Cycle Time and Associated Costs

Raghav Mittal[1], Anand Senguttuvan[1,2], Saikat Chatterjee[1,2], Atanu Mukherjee[2]

[1]M. N. Dastur & Co. (P) Ltd.
P-17 Mission Row Extension
Kolkata 700013, India
Phone: +913322250500
Email: Raghav.M@dastur.com

[2]Dastur Innovation Labs
250 Yonge Street, Suite 2201
Toronto, ON M5B 2L7, Canada
Phone:+(1) - 647-6-DASTUR, +(1) - 647-632-7887
Email: Chatterjee.Saikat@dastur.com

Keywords: Desulphurization, Online Process Control, Ladle Resource Optimization , Ridge Regression, Neural Network

INTRODUCTION

High Sulphur content is detrimental to the mechanical properties of steel. Though the degree of undesirability varies over different grades, the general attempt is to minimize it and avoid the phenomenon of 'hot shortness'. This is caused by the formation of the eutectic Iron Sulphide (FeS). Segregating to the iron grain boundaries, Iron Sulphide decreases the inter-granular strength. As a consequence, by raising the stress levels, it leads to processing related issues such as the formation of cracks during solidification.

Desulphurization or sulphur removal is carried out at multiple stages in the steelmaking process, as depicted in Figure 1. The primary source of Sulphur in the refining procedure is coking coal. A significant percentage (~75%) of the initial Sulphur is removed by moving to the slag phase during reduction carried out in the Blast Furnace. Following the Blast Furnace treatment, an exclusive hot metal desulphurization step is executed in the torpedo. Here, the reagents lime and/or calcium carbide are injected via a lance with nitrogen as a carrier gas[2]. This aids in dropping the Sulphur percentage of the bath, to approximately the desired level for several high-Sulphur tolerant grades but not all.

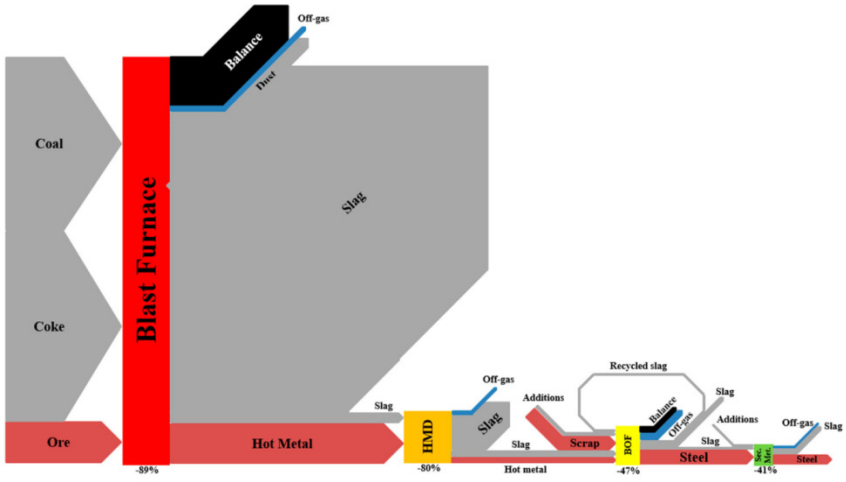

Figure 1. Sources and sinks of sulphur across the BF-BOF steelmaking route at Tata Steel Ijmuiden in 2015. [2]

Structural steel grades are tolerant of Sulphur levels greater than 150 ppm, rendering no requirement for another enhanced Sulphur removal procedure. However, for grades such as ball bearing steels, UHSS, wheels and tube steels the targets are much more stringent. Acceptable levels in these cases can go as low as 10-20 ppm. Low Sulphur content provides high fatigue strength for ball bearing steels while it enhances the resistance to ductile tearing in UHSS, wheels and tube steels[1]. Fine adjustments of such stringent compositions are economically viable only in secondary steelmaking operations carried out in gas stirred ladles.

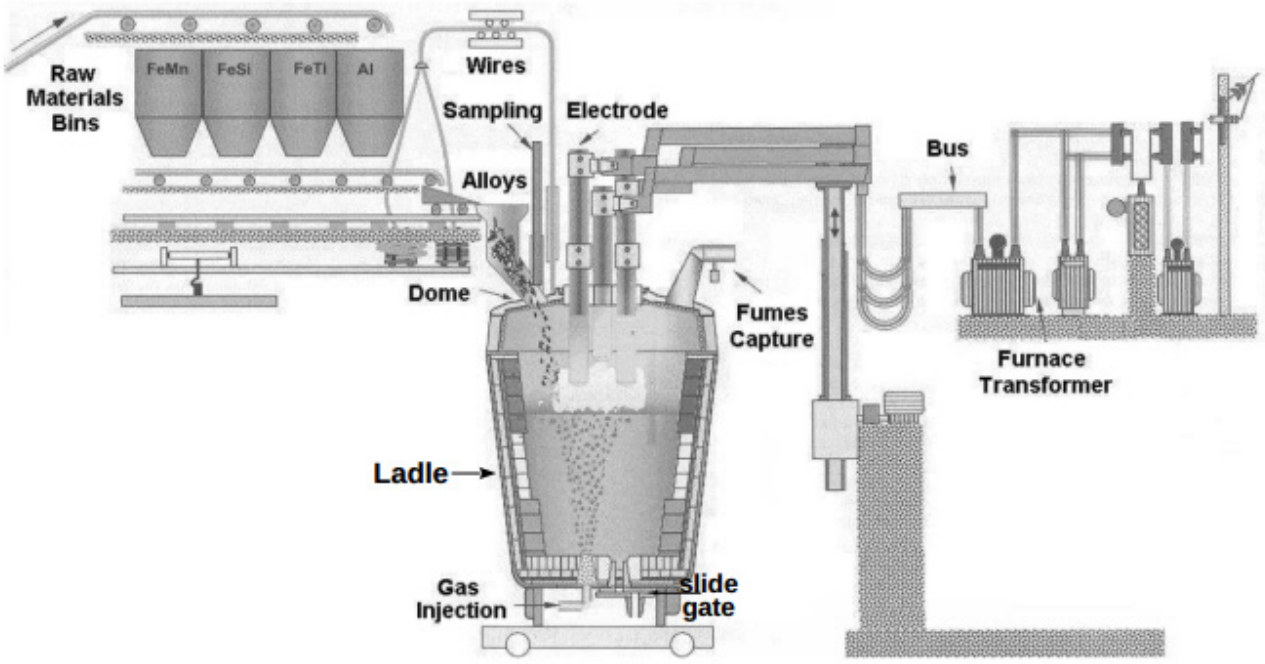

Figure 2. Ladle furnace station showing gas stirred ladle supplied with electric arc heating and power supply systems (right) and alloying addition systems (left) [12]

Ladle operators across the spectrum require some method to track the progress of a heat and take decisions accordingly. Currently, they rely on heuristics and sparse sampling procedures to assess the steel bath. The objective of this paper is to put forward a data-driven predictive model and help operators monitor the heat. The existing practice relies on sampling the heat and determining the composition via chemical analysis. This method is both time-consuming and not precisely on-line. It indicates the bath state at the time of sampling, which lags behind analysis by around 2- 4 minutes. The model suggested helps to bridge this time lag and gain a reasonable understanding of the current bath state. Other compelling reasons for deploying this model in steel plants include:

Reliable Process Operations regardless of the grade
High variation in quality of ore/flux additions in the steps before ladle treatment causes considerable fluctuations in the bath's initial Sulphur content. Consequently, relying on an operator's heuristics to address this variability for different grades may not give as accurate results. Predictive models overcome this issue by accounting for these variations and determining their influence precisely.

Improved steel quality with better process control
Target composition can be achieved with greater confidence if the sulphur trajectory is known throughout a heat and not just for a few intermediate points.

Increased transparency of the process
Although current understanding of the degree of influence that each process parameter individually exerts is reasonably well-known, the correlation between these non-linearly interacting parameters requires further rigorous study. Analysing the massive data available through machine learning techniques can show the way.

Reduced energy, flux material and argon consumption

- Fluxing agents must be added in well-calculated quantities for optimum desulphurization, prolonged refractory life and desired slag fluidity. Online monitoring of the bath can help the operator avoid excessive or too less of flux additions. Both have their demerits. While large quantities of lime decrease the slag fluidity slowing down the kinetics, a minimum quantity of lime is required for efficient desulphurization.
- According to current practice, if at the end of a heat the Sulphur level does not qualify the target threshold (based on sample analysis), the operator has to prolong the heat . This requires re-initiating arcing to maintain the desired temperature. These extra steps can be avoided by deploying a precise online bath monitoring system such as the one suggested here, which holds tremendous potential for significant cost reduction.

Several models have been proposed before to predict the trajectory of Sulphur in a ladle. Metsim Model by Peter *et al.*[3], Coupled Reaction Model by Graham and Irons[4], Coupled Reaction Model by Harada *et al.* [5] are some that based their predictions on a first principles approach. They used Thermodynamics and Kinetics to compute the mass transfer coefficients, slag's sulphide capacity and slag interfacial area to capture the degree of desulphurization reaction. On a similar note, Van-ende *et al.*[6] used FactSage macro processing to develop a kinetic process model while Cao *et al.* [7], Hallberg *et al.*[8] and Singh *et al.*[9] considered CFD analysis for investigating the slag-metal interactions caused by agitation of the bath. All these models have their shortcomings. They remain challenged by the nonlinearity of a ladle's physical and chemical reactions. The correlations between desulphurization kinetics and ladle (both bath and slag) components vary over different grades, flux characteristics (for e.g., quality and size distribution) and addition profiles, carryover slag weight and refractory health. All these factors cumulatively contribute to the stochastic nature of the process which these models are not able to capture. Secondly, these first principles based models lack the flexibility to be open to modifications from practical data and learn with time.

To accommodate the factors mentioned above and address the need for robustness by constantly learning from practical data, an on-line machine learning based predictive model has been developed for monitoring ladle desulphurization. This model determines the current trajectory of bath elements (sulphur, in this case) without the need for probing the heat by taking slag and bath samples.

METHOD

Thermodynamic and Kinetic Considerations

Sulphur removal in the ladle takes place can be expressed via the ionic reaction given by Holappa *et al.*[15] below.

$$[S] + (O^{2-}) = [O] + (S^{2-}) \quad (1)$$

$$[S] + (CaO) = [O] + (CaS) \quad (2)$$

where ( ) indicates species in the slag phase, and [ ] for species in the steel bath. In practice, this oxide ion is provided by the Calcium Oxide from the slag. Sulphur dissolved in the bath displaces oxygen in lime during slag-metal emulsification driven by argon purging. Hence, sulphur is absorbed by the slag as it forms Calcium Sulphide (CaS). From the Eq. (1) and (2), the thermodynamics of the reaction is influenced by both the slag basicity and the bath's oxygen potential. While higher basicity (not too high either as it would affect slag fluidity) provides a higher driving force, a higher oxygen potential has a tendency to re-sulphurize the bath. Therefore the following derived quantities were considered for determining their cumulative influence on the desulphurisation process.

Basicity

Binary Basicity $B_{1,}$ $$B_1 = (CaO) / (SiO2) \quad (3)$$

Quaternary Basicity: $$B_2 = ((CaO) + (MgO)) / ((SiO2) + (Al2O3)) \quad (4)$$

Optical Basicity B_{op} : $$\Lambda = \Sigma X_i \Lambda_{i,} \quad (5)$$

where Λ is the optical basicity of the slag and Λ_i is the optical basicity of individual oxides and

$$X=\frac{mole\ fraction\ of\ component*number\ of\ oxygen\ atoms\ in\ oxide\ molecule}{\Sigma\ mole\ fraction\ of\ component*number\ of\ oxygens\ in\ oxide\ molecules\ of\ all\ components}$$

Oxygen Potential

Carry-over slag from the Basic Oxygen Furnace introduces easily reducible oxides FeO and MnO into the ladle slag. Owing to their ability to reoxidize the bath, high quantity of these oxides tends to retard the desulphurization process.

$$L_s = 26.8811 - 24.6379\ (\%\ MnO) \quad (8)$$

Through Eq. (8), Bulko *et al.*[13] showed how, statistically, the sulphur distribution ration (L_s) decreases with rise in the weight percentage of MnO, which signifies an increase in the oxygen potential of the bath. Bearing this in mind, we took into consideration the weight of these oxides in the slag for including the role played by oxygen potential.

Rate Constant

From the past work, it is well known that the kinetics of the process is largely governed by the fluid flow phenomenon. Argon stirring of the bath greatly increases the slag-metal interfacial area through slag entertainment, leading to enhanced kinetics[14]. Accordingly in Figure 3, it is seen that the rate parameter (mass transfer capacity coefficient) is mostly a function of stirring power (due to gas injection), despite the scatter in the plot, which can be attributed to the variations in steel grade and mass of carry over slag.

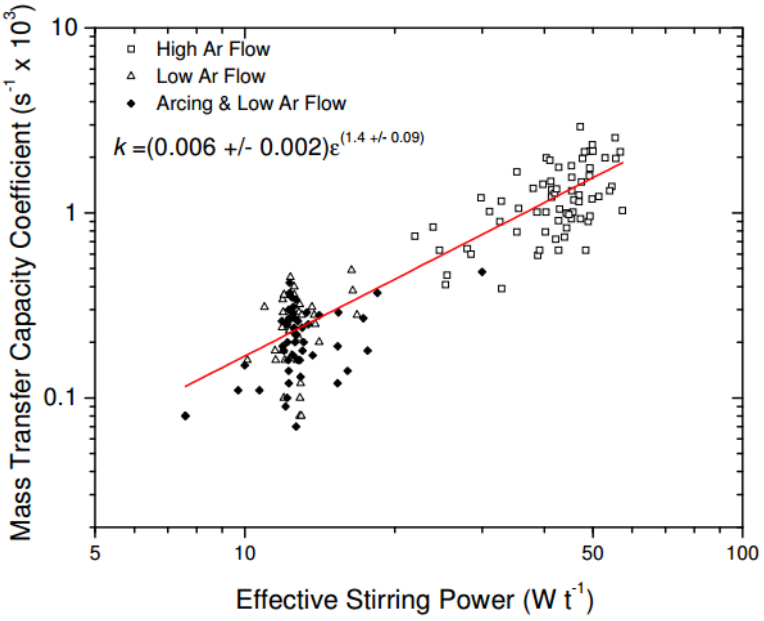

Figure 3. Relationship between mass transfer capacity coefficient and effective stirring power [14]

Model Development

The predictive model developed is based on the 41 heat dataset from PhD thesis of Graham[14]. Further, Graham had developed a rigorous kinetic model based on first principles to predict the trajectory of bath and slag components. He computed those based on the argon purging profile, flux additions and the electrical energy provided via arcing. Here, however, to further enhance the predictability and make it robust for multiple grades, a data-driven approach has been adopted. The 41 heat data set was split into a training set comprising 32 heats and a test set comprising eight heats after eliminating an outlier (based on the initial and final bath composition). This data was recorded at the Steel Melt Shop of ArcelorMittal, Dofasco. Furthermore, the dataset is not unique to a particular grade of steel instead; it accommodates multiple grades. An exploratory data analysis of the initial and final bath composition reveals the same.

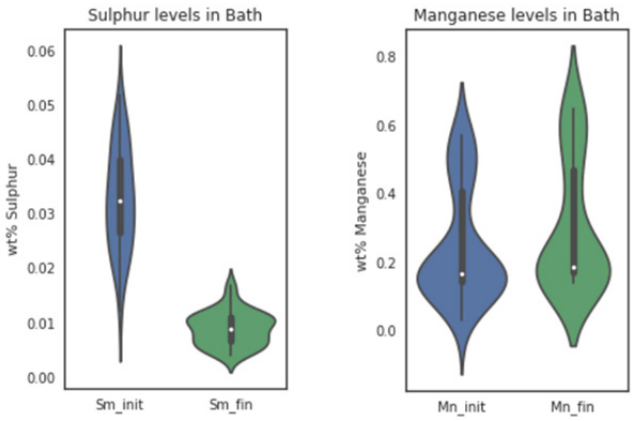

Figure 4. Violin plots of the initial and final levels of sulphur, manganese in the steel bath.

For plotting both, the spread and the probability density of data at different values, we carried out data visualisation using Violin plots. The bath as well as the slag composition were observed over the 40 heats. This exercise assisted in drawing the constraints of the dataset, summarizing it visually and gauging the degree of variation in each variable. The following figures depict the vertical spread and density of values in the individual elements of bath and components of slag before and after a heat. Since the slag composition was not found to vary much over a heat, the final slag composition has been ignored. Figure 4 depicts the large variation in initial sulphur levels as the range is defined by a minimum of 120ppm and a maximum of 520ppm. The final sulphur levels, on the other hand, lie within a narrower range of 40-170ppm.

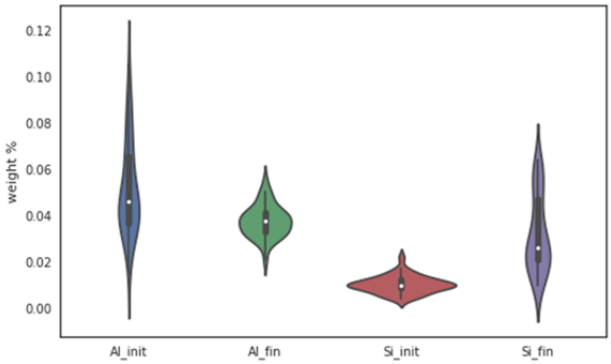

Figure 5. Violin plots of the initial and final levels of aluminium and silicon in the steel bath

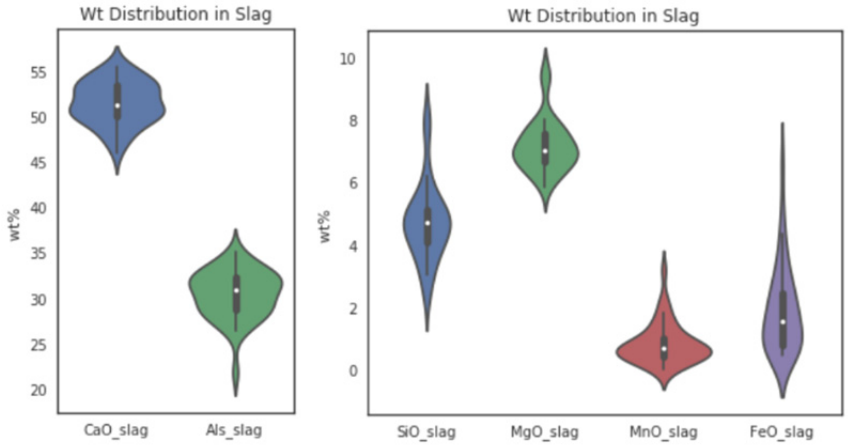

Figure 6. Violin plots of the initial levels of CaO, Al_2O_3, SiO_2, MgO, MnO and FeO in slag.

Similarly, Figure 6 shows the large spread in the initial FeO and MnO content of the slag phase. Ranging in between 0.5-6.6 wt% and 0.66-3.22 wt% respectively, the values clearly reflect the high uncertainty in the weight of carryover slag; which contributes to higher oxygen potential.

A typical heat has been captured in the following format in the PhD thesis of Graham[14]. Figure 7 plots the argon purging profile, total units of electrical energy provided via arcing, instances of flux additions (without any mention of the quantity added) and the sampling instances. Figure 8(a) on the other hand has captured the element-wise composition of the bath corresponding to the instances when sampling was carried out. Similarly, Figure 8(b) shows us the variations in slag component over a given heat. In Figure 8(a) and (b), the markers depict actual sampling results while the continuous lines are the predictions of Graham's kinetic model.

To make the model relevant to the real shop-floor scenario, only the initial bath and slag composition were considered along with the controllable parameters that an operator dictates. The motivation behind this is to do away with any intermediate sampling for monitoring the steel bath. From graphs like the ones in Figure 7 and 8, for each of the 40 heats, relevant data was extracted after performing the necessary sanitization. To assess the contributing factors for ladle desulphurization process, derived quantities mentioned earlier were computed subsequently. All input variables can thus be categorised as follows:

1. *Data Parameters*: argon purging flow rate, bath composition samples (min 5 over the entire heat), initial slag composition, flux addition profiles (only their time instances and not their amounts), temperature.
2. *Derived quantities*: total volume of argon purged, mean of argon flow rate to gauge the intensity of purging, standard deviation of argon purging flow rate (to capture the spread around the mean), difference in sulphur level over the entire heat, slag basicity (B_1, B_2, and B_{op}), sulphide capacity of slag.

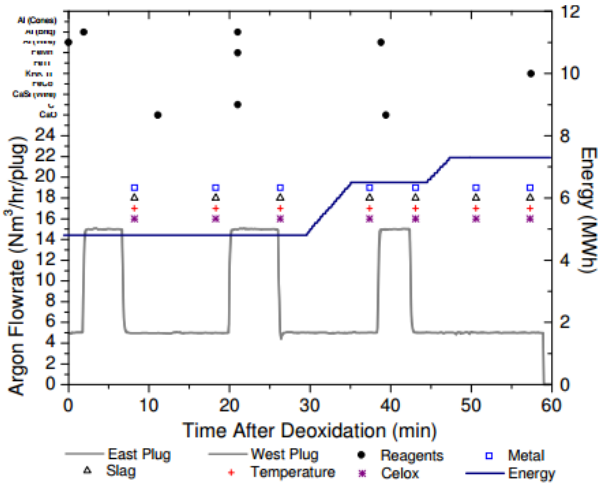

Figure 7. Argon purging, flux addition and electrical heating energy profile [14]

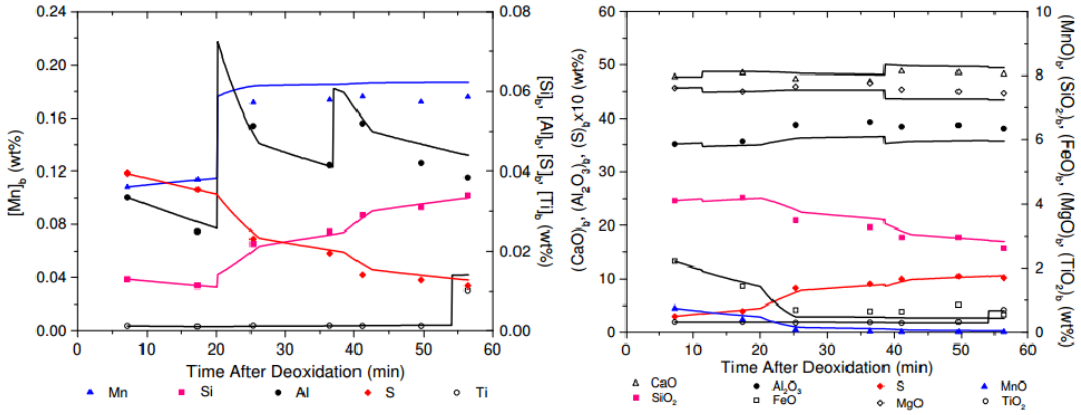

Figure 8. (a) Element-wise composition details of the liquid steel bath (markers depict the sampling results throughout the heat. (b) Composition of individual components of the slag[14]

Table 1. All input variables for the model along with the target variable, sulphur difference

Vol. of Argon Purged (Nm^3)	Ar_total_vol
St. Dev. of Ar Flow Rate (Nm^3/hr)	Ar_rate_std
Mean of Ar Flow Rate (Nm^3/hr)	Ar_rate_mean
Vol. of Ar purged>5 Nm^3/hr	Ar_high_vol
Time taken by heat	Heat_time
Initial Sulphur content in steel bath	Sm_init
Initial Aluminium in bath	Al_init
Initial Silicon in bath	Si_init
Initial Manganese in bath	Mn_init
Initial CaO in slag	CaO_slag
Initial SiO_2 in slag	SiO_slag
Initial MgO in slag	MgO_slag
Initial MnO in slag	MnO_slag
Initial FeO in slag	FeO_slag
Basicity B1	basicity_1
Quaternary Basicity B2	basicity_2
Optical Basicity	basicity_op
Sulphide Capacity	Cs
Difference in Sulphur	Sm_diff

Assumptions of our model include:

- Liquid bath is isothermal, i.e. the minor variations in temperature are not significant enough for kinetic considerations. Instead, kinetics is determined mainly by slag-metal emulsification.
- Electrical heating energy provided by arcing does not play a considerable role either, as the extent to which it affects temperature change can be disregarded for the reason mentioned above.

Having set the assumptions, the optimum combination of features was decided based on their correlation matrix mapping (both predictors and target) against each other and an analysis of the R^2 values obtained from the different combinations. A heat map of the Pearson's correlation coefficients was investigated to visualise the correlation matrix.

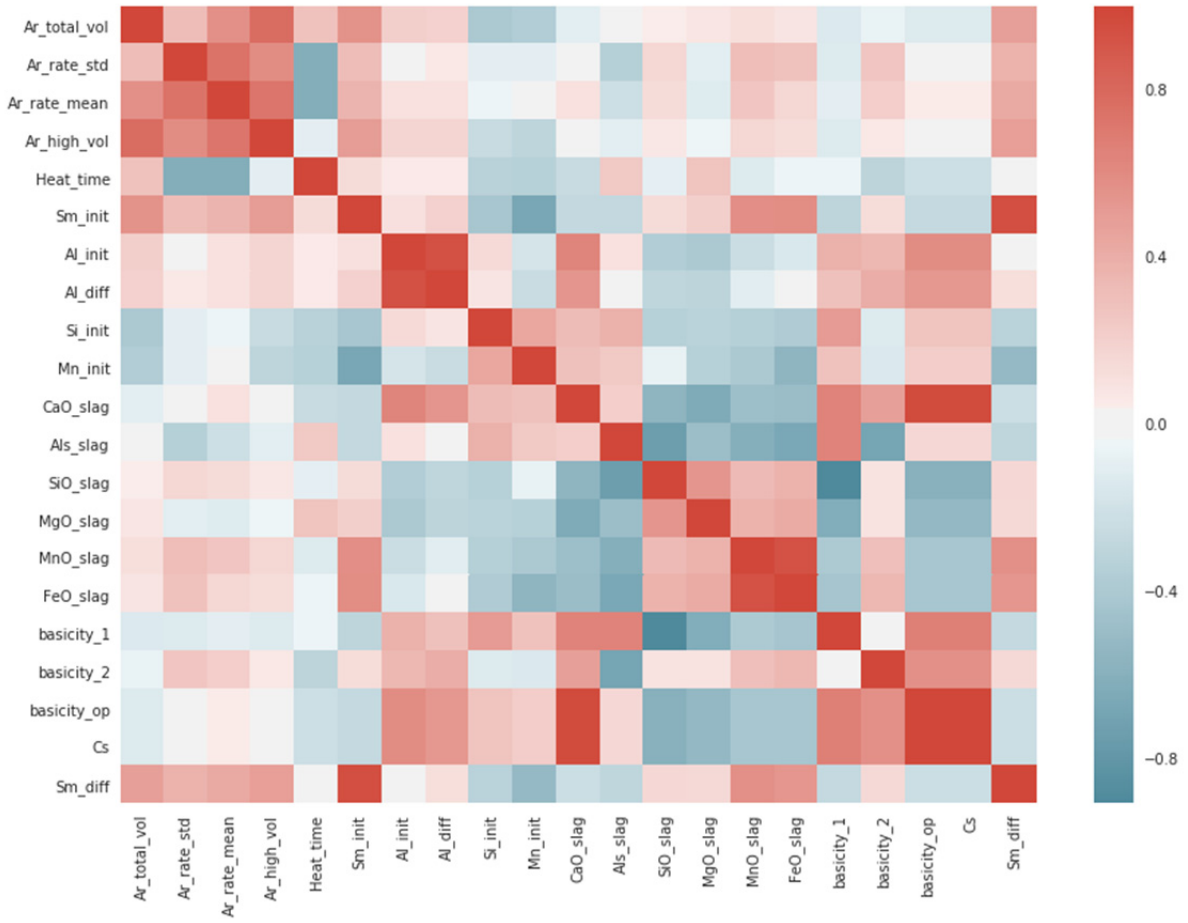

Figure 9. Heat map of Pearson correlation coefficients of the predictors and the target variable.

Based on the Pearson correlation coefficients of predictors with the target (*Sm_diff*), the individual influence of each predictor was analysed. This gave a fair idea of how the target was affected independently by every feature but it did not capture the interactions in between them. Therefore, to account for the multi-colinearity effect on the target, cumulative influence (i.e. model's R^2 values) of different combinations of variables was scrutinized to find the optimum set of features.

Model Flow

As mentioned earlier an arbitrary set of eight heats was shortlisted and isolated from the training heats for testing the model's performance. From the thirty-two training heats, six (~20%) were utilized for cross-validation. The sampling results of both steel and slag phase were then piece-wise linearly interpolated for the 32 training heats giving us trajectories for training the model. Following this interpolation procedure, each training set heat was sub-divided into one minute time steps giving approximately 40 steps per heat i.e. around 1200 steps in total. Derived quantities listed above were computed (for all the time steps) and appended to the set of predictors. Each predictor variable from the training set was then normalised (mean-centred & standard deviation scaled) to address the distortion in the predictors' vector space. Later however, normalisation for the test heats, was carried out using the metrics (mean and standard deviation) generated from the training set.

The model was then trained based on two machine learning algorithms discussed in the 'Algorithm Selection' Section.

Dynamic prediction of the bath's sulphur content necessitates an assessment of both the current time step and the previous one for gauging the extent of desulphurization reaction. Marching with time, after training the model with 5-fold cross-validation, the sulphur trajectory for test heats was predicted and augmented with every time step.

Beginning with the initial composition (bath and slag) for each test set heat, the model first computed the change in sulphur level for the first minute. This value was used to calculate the current step's final sulphur level and the next step's initial sulphur level, both of which are the same. Similarly, for the step that followed, change in sulphur was computed with the initial sulphur value obtained from the step that preceded it. In this fashion, as the heat progressed, the model gave its approximation of the path traced for determining the steel bath's sulphur level.

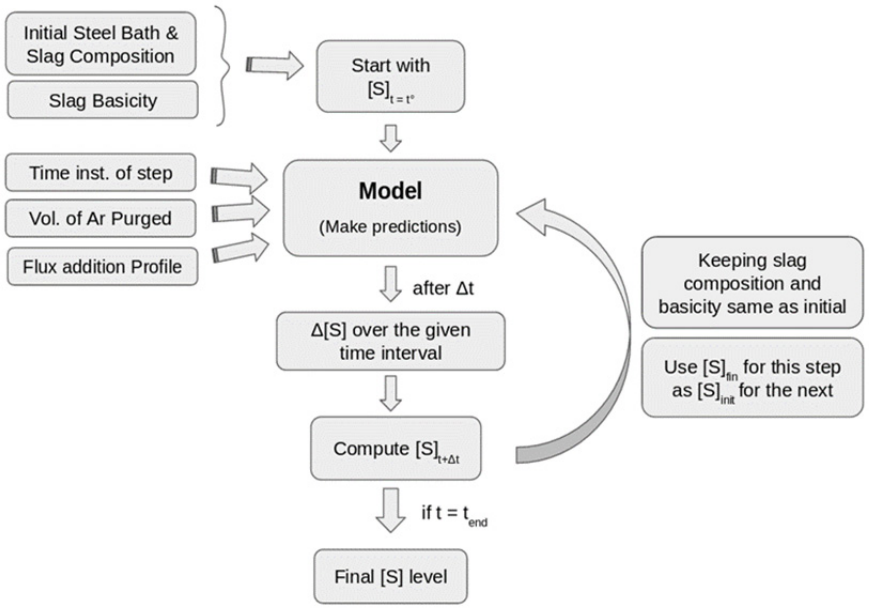

Figure 10. Flow diagram representing the dynamic prediction of sulphur for every time step (one minute here).

The crucial thing to note here is that this model does not require composition details from either the slag phase or the steel bath for any of the intermediate steps in a heat. Hence, it can be easily deployed alongside real-time operations to gain online insights regarding the current sulphur level.

Algorithm Selection

Two different methods were used to predict the sulphur trajectory of the test heats: 1. Ridge Regression (Multivariate Linear Regression with Regularization) and 2. Neural Networks.

Ridge Regression

Essentially, ridge regression is a multivariate-linear regression technique that is coupled with $\boldsymbol{l_1}$ regularization[17]. It penalizes coefficients of predictor variables thereby assigning them weights based on their influence on the optimization process.

$$\sum_{i=1}^{M}(y_i-\hat{y}_i)^2=\sum_{i=1}^{M}\left(y_i-\sum_{j=0}^{p}w_j\times x_{ij}\right)^2 \tag{9}$$

$$\sum_{i=1}^{M}(y_i-\hat{y}_i)^2=\sum_{i=1}^{M}\left(y_i-\sum_{j=0}^{p}w_j\times x_{ij}\right)^2+\lambda\sum_{j=0}^{p}w_j^2 \tag{10}$$

where, w_i represents the coefficients of each of the features of the multivariate linear model, x_{ij} the value of the j^{th} predictor variable of the i^{th} data point, y_i the real value of the target, $\hat{y}$ the predicted value of the target and λ, the regularization parameter . So, while Eq. (9) gives the cost function for a simple linear model, Eq. (10) shows the method for computing the cost function for ridge regression. The minimization of this cost function gives us an optimized set of coefficients for regression.

Neural Networks

Based on the architecture of neural connections in our brains, neural networks are believed to be a simulation of the way humans learn from experience. They are capable of capturing non-linearity in better ways than Ridge regression.

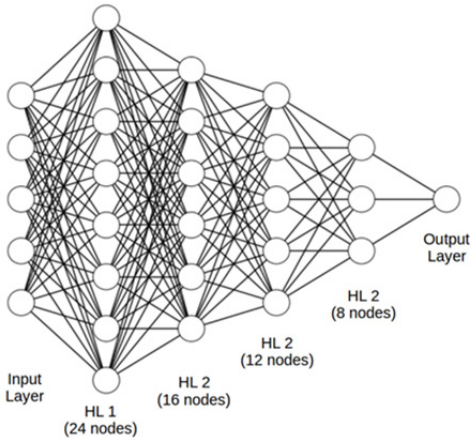

Figure 11. Optimum architecture of the Neural Network for our analysis (HL: Hidden Layer).

Different combinations of network architecture were attempted by varying the number of nodes, number of layers, the learning rate and the activation function to optimize the model's learning ability. The best results were obtained with the model architecture represented in Figure 11.

RESULTS AND DISCUSSION

R^2 values or the coefficient of determination of the two algorithms were used as the metric to assess model performance. As mentioned earlier, in order to overcome the train-test split bias, 5-fold cross-validation was carried out thereby ensuring an arbitrary split. The findings are discussed below:

Ridge Regression

A grid of values of the regularization parameter *lambda* (λ) was created to ascertain the optimum value which gave minimum average cross-validation scores. Figure 12(a) shows the variation in the CV scores with *lambda* (λ), described in Eq. (10). On the other hand, Figure 12 (b) is a scatter plot of the predicted and real Sulphur differences. The sulphur differences plotted are over all the one minute time steps of the test heats. The predicted Sulphur trajectories for some test heats are shown in Figure 13.

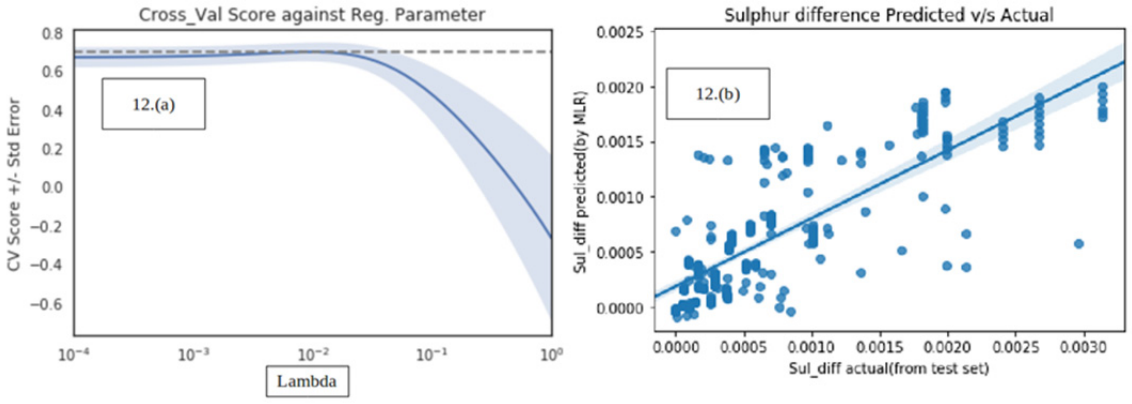

Figure 12. (a) Variation of Cross-Validation Score with the regularization parameter. (b) Scatter plot of predicted and real Sulphur differences of all 1min time steps from the test heats.

Figure 12(b) show the degree of accuracy of the model's predictions on the test set. Best results were obtained with a value of 10^{-2}(0.01) for the regularization parameter λ. Among the eights test heats chosen, predictions for the three depicted in Figure 13 gave the best results. Despite being reasonable in its approximations (average 5-fold cross-validation score of 0.66 for sulphur differences over the test heats' time steps), the trajectories computed by the model have certain shortcomings: 1. They tend to show deviation (a higher gradient than expected) towards the end of the process and 2. The Sulphur differences show a lag before sudden change in gradient. These errors can be attributed partially to the nature of the dataset. The forty heats analysed are not only a few in number but also comprise a variety of steel grades. Information regarding the grade

details wasn't mentioned in Graham's thesis[14] and no clustering procedure was carried out to identify them as it would have further reduced the scope of the model's learning ability. The authors are, however, confident that given a larger dataset with requisite features, the course of desulphurization can be predicted with higher accuracy.

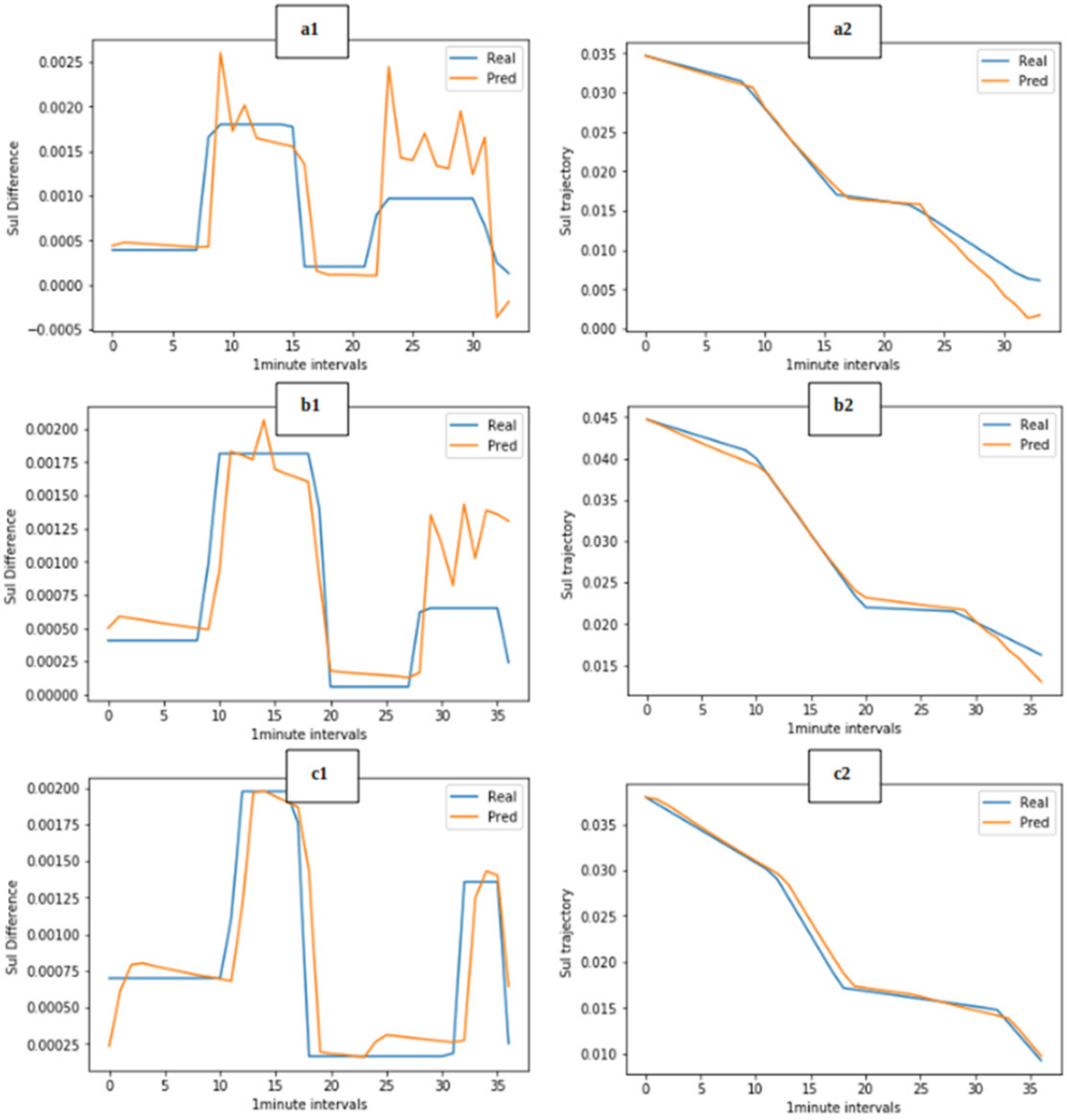

Figure 13.Sulphur difference(1) over each time step and sulphur trajectory (predicted v/s real)(2) for heat numbers 23, 4 and 37 marked as **a**, **b** and **c** respectively as predicted by Ridge Regression

Neural Networks

As Table 2 and Figure 15 depict, an average 5-fold cross-validation score of 0.675 was obtained for sulphur differences over the test heats' time steps. This is marginally better than what we observed for Ridge Regression. Contrary to the conclusions from the R^2 values for the two models, we see that the trajectories are better than Ridge Regression. This should not misguide us for the overall performance of the neural networks because the Sulphur curves shown here are for three best heats from an arbitrary test set. They do not reflect the model's accuracy over all 5 arbitrary test sets based on which the R^2 value has been computed.

Table 2. R^2 values of the models over 5 distinct and arbitrary cross-validation folds.

Model	R^2_1	R^2_2	R^2_3	R^2_4	R^2_5	Avg CV Score	R^2 for Test set
Ridge Regression	0.523	0.672	0.833	0.832	0.440	0.660	0.648
Neural Networks	0.542	0.634	0.792	0.776	0.630	0.688	0.675

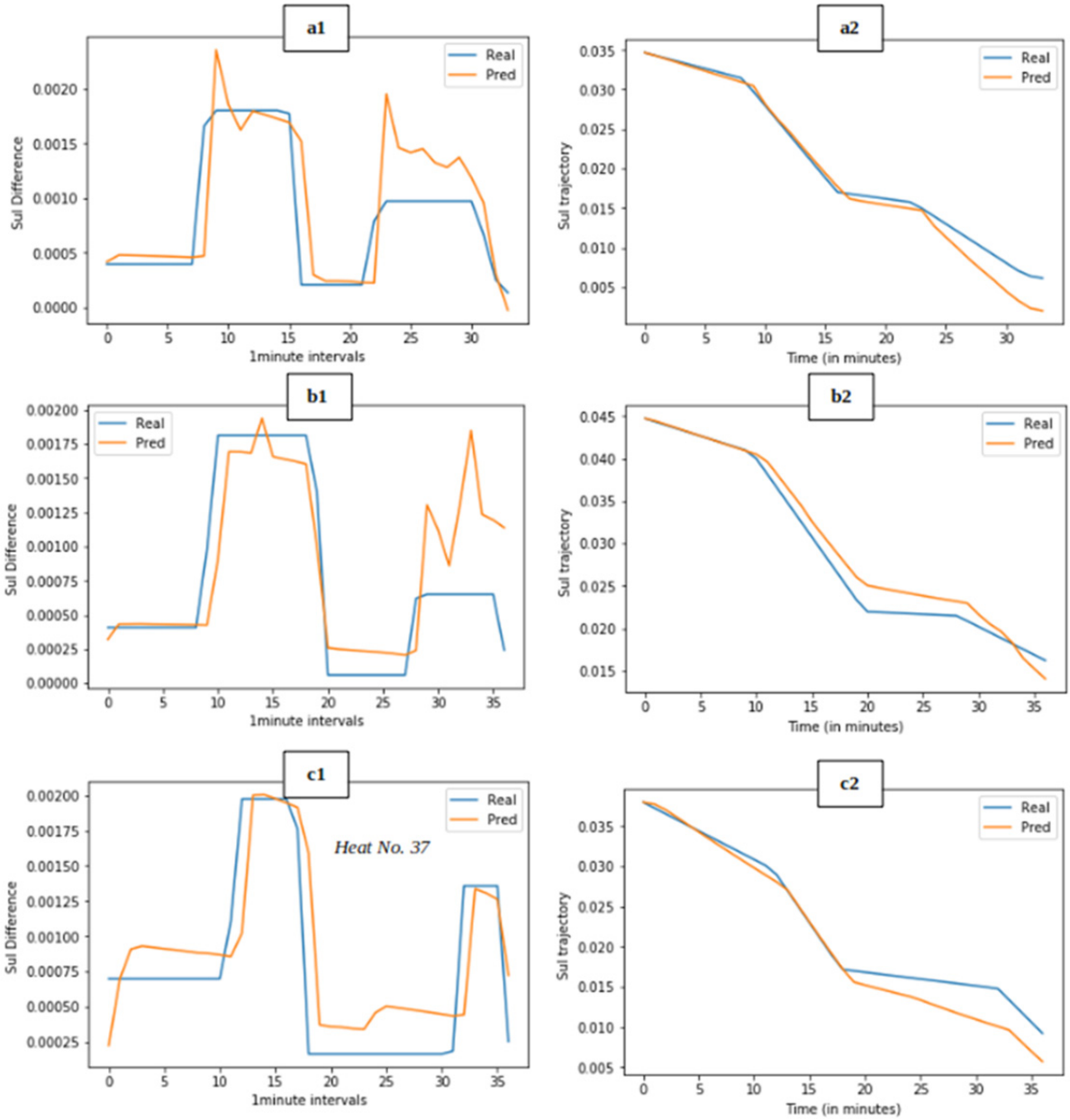

Figure 14. Sulphur difference(1) over each time step and sulphur trajectory (predicted v/s real)(2) for heat numbers 23, 4 and 37 marked as **a**, **b** and **c** respectively as predicted by Neural Networks

Investigating the sulphur trajectories in Figure 14 further reveals that the model suffers from the same issues as the previous learning technique. The predictions are more chaotic and higher than expected towards the end of a heat. There are two things that could possibly be causing this. One reason here could be the fact that as a heat progresses, the driving force for desulphurization reaction drops because of lower sulphur content in the bath. Since the change in sulphur values is modest, the author's believe that it tends to the order of magnitude of the noise that this process is characterized by. As a consequence, it gives fluctuating and relatively higher values. Another issue observed during exploratory data analysis was that some heats

(~8) showed sulphur reversion/stagnation taking place towards the end. Again, owing to some instances of such contradictory trends in the trajectory, the model wasn't able to capture the latter half equally well.

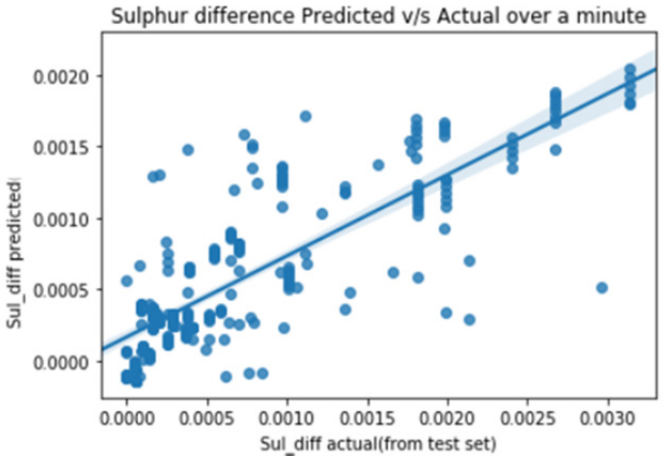

Figure 15. Scatter plot of predicted and real Sulphur differences of all 1min time steps from the test heats.

Other than that, the neural networks were reasonably successful in predicting the sulphur differences over the time steps of a heat despite their magnitudes being of the order of 10^{-4}. Based on such qualified predictions, the model performed well in capturing the shape of the sulphur curves. Here again, we believe that a larger dataset with additional features (flux addition weights, quality of flux, grade of steel, etc.) can enhance the predictability of the model.

Economic Assessment

Integration of this online predictive model with the ladle operations system can help monitor and thus control the evolution of a heat more reliably. For the operators, this model would assist them in ensuring the achievement of quality targets (based on stringent composition demands) under minimum energy, material and production costs. Not only would the ladle run at maximum productivity but also have indirect advantages in the logistics of the plant. Most importantly, the plant would not have to bear the economic burden of downgrading due to a violation of the Sulphur target limits.

Based on the best results from the model, cost-benefit analyses were performed for a 4.5 mtpy steel melt shop having 3 x 150t BOF and 2 x 150t ladle furnaces. As per the current scenario, the absence of an online monitoring system often results in higher re-processing time, frequent caster sequence miss, additional flux material, increased argon consumption, increased electricity consumption(arcing), electrode wear due to longer use and higher percentages of off-grades. Considering the following assumptions of: (a) 0.2% yield improvement in caster with higher sequence (b) average profit margin of 200 US$/ton of additional slab and (c) reduction of processing time by 2-3 minutes with an average of 40 minutes d) improvement in average specific consumption for energy, argon, lime, electrode and refractory, the potential cost savings can range from 5-7 million US$ per annum.

CONCLUSIONS

A dynamic predictive model has been developed for online monitoring of the desulphurisation process in a ladle. Machine learning techniques, Ridge Regression and Neural Networks, were used for analysing a dataset from ArcelorMittal, Dofasco[14]. For ensuring robustness of approach, the idea was to come up with a tool which can be utilised by operators for exercising better control over the steel bath composition. The model, therefore, aims at eliminating intermediate sampling of the bath for probing the progress of a heat. The model is found to give reasonably accurate predictions for sulphur differences over one minute time steps despite their order of magnitude being as low as 10^{-4}. Based on the precise computation of sulphur differences, the model was successful in capturing the shape of sulphur trajectories.

In addition, upon integration with real-time operations, the suggested model holds tremendous potential to optimize ladle heats by reducing the processing time, product off-grades and consumption of flux, argon and electricity. Economic assessment showed that cumulatively these factors can contribute to significant savings on the production front.

REFERENCES

1. Nadif, M., J. Suero, C. Rodhesly, D. Salvadori, F. Schadow, R. Schutz, E. Perrin, and L. Peeters. "Desulfurization practices in ArcelorMittal flat carbon Western Europe." *Revue de Métallurgie–International Journal of Metallurgy* 106, no. 7-8 (2009): 270-279.
2. F. N. H. Schrama, E. M. Beunder, B. V-der Berg, Y. Yang and R. Boob, "Sulphur removal in ironmaking and oxygen steelmaking," *Ironmak. Steelmak.*, Vol. 44, No. 5, 2017, pp. 333-343.
3. J. Peter, K.D. Peaslee, D.G.C. Robertson, and B.G. Thomas: Proc. AISTech, 2005, vol. 1, pp. 959–73
4. K.J. Graham and G.A. Irons: Iron Steel Technol., 2009, vol. 6, pp. 164–73.
5. A. Harada, N. Maruoka, H. Shibata, and S. Kitamura: ISIJ Int., 2013, vol. 53, pp. 2110–17
6. M.-A. Van Ende, Y.-M. Kim, M.-K. Cho, J.H. Choi, and I.-H. Jung: Metallurgical and Materials Transactions B, 2011, vol. 42, pp. 477–89
7. Cao, Q., Pitts, A., Zhang, D., Nastac, L. and Williams, R., 2016. "3D CFD...Desulfurization Kinetics. In *Advances in Molten Slags, Fluxes, and Salts*: Proceedings of the 10th International Conference on Molten Slags, Fluxes and Salts 2016 (pp. 1009-1016). Springer, Cham.
8. Andersson, Margareta, Malin Hallberg, Lage Jonsson, and Pär Jönsson. "Slag-metal reactions during ladle treatment with focus on desulphurisation." *Ironmaking & steelmaking* 29, no. 3 (2002): 224-232.
9. Singh, U., Anapagaddi, R., Mangal, S., Padmanabhan, K.A. and Singh, A.K., 2016. Multiphase modeling of bottom-stirred ladle for prediction of slag–steel interface and estimation of desulfurization behavior. *Metallurgical and Materials Transactions B*, *47*(3), pp.1804-1816.
10. R.J. Fruehan: The Making, Shaping and Treating of Steel, 11th ed., The AISE Steel Foundation, Pittsburgh, 1998, p.661.
11. S. Asai, M. Kawachi, and I. Muchi, Proceedings, Scaninject III, part I (1983): 12:1.
12. Sampaio, Patricia Teixeira, Antonio Padua Braga, and Takeshi Fujii. "Neural network thermal model of a ladle furnace."
13. *Engineering Applications of Neural Networks* 284 (2007): 80-86.
14. Bulko, B., J. Kijac, and T. Borovský. "The influence of chemical composition of steel on steel desulphurization." Archives of Metallurgy and Materials 56, no. 3 (2011): 605-609.
15. Graham, Kevin James. "Integrated Ladle Metallurgy Control." PhD diss., 2008.
16. L. Holappa:'Secondary steelmaking'.In: S. Seetharaman, editor.Treatise on process metallurgy: industrial processes. Oxford, Elsevier, 2014, 301–345.
17. Bathy, K., and V. Math. "Optimization of Steel Production: Ladle Furnace Slag and Caster Productivity." Department of Mechanical Engineering Mcgill university Montreal, Canada (December 2012) (2012).
18. Hoerl, Arthur E., and Robert W. Kennard. "Ridge regression: Biased estimation for nonorthogonal problems." *Technometrics* 12, no. 1 (1970): 55-67.

